

Evidence for pH dependent Zn^{2+} influx in K562 erythroleukemia cells: Studies using ZnAF-2F fluorescence and $^{65}Zn^{2+}$ uptake

Robert A. Colvin^{a,*}, Charles P. Fontaine^a, Dustin Thomas^a,
Tomoya Hirano^b, Tetsuo Nagano^b, Kazuya Kikuchi^b

^a Department of Biological Sciences, OHIO University, Athens, OH 45701, USA

^b Graduate School of Pharmaceutical Sciences, The University of Tokyo, Tokyo, Japan

Received 10 July 2005, and in revised form 17 August 2005

Available online 8 September 2005

Abstract

Using both ZnAF-2F (a Zn^{2+} specific fluorophore) and $^{65}Zn^{2+}$, we determined the rate of transporter mediated Zn^{2+} influx (presumably mediated by the SLC39A1 gene product, protein name hZIP1) under steady state conditions and studied the effects of extracellular acidification. When K562 erythroleukemia cells were placed in Zn^{2+} containing buffers (1–60 μ M), the initial rate of $^{65}Zn^{2+}$ accumulation mirrored the apparent rise in free intracellular Zn^{2+} concentrations sensed by ZnAF-2F. Therefore, newly transported Zn^{2+} equilibrated with the free intracellular Zn^{2+} pool sensed by ZnAF-2F. A new steady state with elevated free intracellular Zn^{2+} was established after about 30 min. An estimate of 11 μ M for the K_m and 0.203 nmol/mg/s for the V_{max} were obtained for Zn^{2+} influx. $^{65}Zn^{2+}$ uptake and ZnAF-2F fluorescent changes were inhibited by extracellular acidification (range tested: pH 8–6, IC_{50} = pH 6.34). The IC_{50} for proton effects was close to the pK_a for histidine, suggesting conserved histidine residues present in SLC39A1 play a critical role in Zn^{2+} influx and are involved in the pH effect.

© 2005 Elsevier Inc. All rights reserved.

Keywords: Metal ion transport; Zinc homeostasis; Fluorescence

Using currently available genomic data and analyses from several eukaryotic organisms, Zn^{2+} transporters appear to fall into two distinct gene families named SLC39 (protein name: ZIP) [1,2] and SLC30 (protein name: ZnT) [3]. Functional characterization of the mammalian SLC39 family members (hZIP-1, -2, and -4) provides convincing support for the notion that SLC39 proteins are targeted to the plasma membrane and are involved primarily in cellular Zn^{2+} influx [4–7]. SLC39 proteins appear to mediate a facilitated diffusion of Zn^{2+} , driven primarily by the concentration gradient for Zn^{2+} across the plasma membrane. No evidence exists for an energy requirement, effect of membrane potential, or the cotransport of other ions, except perhaps bicarbonate (SLC39A2 only) [4,5]. Thus, very little

is known concerning the mechanism of Zn^{2+} influx. One recent study suggests that SLC39 proteins move ligand bound Zn^{2+} across the plasma membrane (rather than free Zn^{2+}) [8], the implication being that Zn^{2+} added in solution is a poor measure of the protein's true affinity for Zn^{2+} .

The function, tissue location, and mechanism of Zn^{2+} transport by SLC30 family members are best studied for the product of the mammalian gene SLC30A1 (ZnT-1) and its several homologs. [9]. SLC30A1 is ubiquitously expressed and likely to be involved in Zn^{2+} efflux. For example, PC-12 cells expressing SLC30A1 show increased Zn^{2+} efflux and reduced sensitivity to Zn^{2+} induced cell death [10]. The remaining SLC30 family members are preferentially localized to intracellular membranes where they have more limited, tissue specific expression, probably related to physiological intracellular Zn^{2+} compartmentalization [11–16]. Several studies [5,9,14–16] support a division of labor between Zn^{2+} transporters. Thus, SLC39 family members

* Corresponding author. Fax: +1 740 593 0300.

E-mail address: colvin@ohio.edu (R.A. Colvin).

are responsible for Zn^{2+} influx and SLC30 family members are involved in Zn^{2+} efflux and intracellular compartmentalization. This leads to a model predicting that under steady state conditions, free intracellular Zn^{2+} concentrations are maintained by a balance between the rate of separate and distinct Zn^{2+} influx and efflux mechanisms across the plasma membrane and exchange with sequestered Zn^{2+} pools inside the cell. However, direct experimental proof of this model in mammalian cells is lacking at present.

Our laboratory is studying Zn^{2+} transport using cultured cells in hopes of addressing questions of transport mechanism and the role of mammalian Zn^{2+} transporters in cellular homeostasis. One of our consistent findings is an inhibition of $^{65}Zn^{2+}$ uptake by extracellular acidification. In addition, we have shown that intracellular acidification of cortical neurons results in a stimulation of $^{65}Zn^{2+}$ uptake [17,18]. These data have led us to hypothesize that protons are fundamental to the uptake mechanism and the pH effect could reflect an antiport mechanism of coupled Zn^{2+} /proton transport. Unfortunately, no experimental evidence exists linking protons to the transport mechanisms of either SLC30 or SLC39 family members. To address issues of cellular Zn^{2+} homeostasis and the mechanism(s) of Zn^{2+} transport, we used a model cell system (K562 erythroleukemia cells) with well characterized Zn^{2+} uptake transporter function and two complimentary techniques—ZnAF-2F fluorescence and $^{65}Zn^{2+}$ uptake. These studies allowed us to measure initial rates of Zn^{2+} influx and measure changes in steady state intracellular Zn^{2+} levels. Our data suggests that SLC39A1 (hZIP1) transport function was inhibited by extracellular acidification.

Materials and methods

Culture of K562 erythroleukemia cells

K562 erythroleukemia cells (#CCL-243) were obtained from American Type Culture Collection (Manassas, VA). Cells were maintained in complete RPMI 1640 medium (Life Technologies), supplemented with 2 mM glutamine and 10% fetal bovine serum (Atlas Biologicals, Fort Collins, CO) with 500 ng/ml Gentamicin and 250 ng/ml Fungizone (Life Technologies) added. Cells were grown in suspension in 25 cm² flasks at 37 °C in a 5% CO₂ incubator. When necessary, cells were allowed to attach to poly-D-lysine (0.1 mg/ml in borate buffer) coated coverslips overnight. Approximately, 5×10^4 cells were applied to each coverslip. This quantity of cells per coverslip provides an optimal fluorescent signal when using ZnAF-2F.

$^{65}Zn^{2+}$ flux measurements

Experiments were performed similar to those described previously [17]. K562 cells were first harvested by centrifugation (5 min at 500 rpm—Beckman Allegra 25R centrifuge) and then resuspended in Locke's buffer (154 mM NaCl, 5.6 mM KCl, 2.3 mM CaCl₂, 1.0 mM MgCl₂, 5 mM Hepes, and 10 mM glucose). The cell suspension was then assayed

for protein by the Bio-Rad method using bovine serum albumin as the standard. The cells were then diluted to a concentration of 1.5–2.0 mg/ml. Locke's buffers (bubbled with O₂ to remove dissolved CO₂) containing $^{65}Zn^{2+}$ (Los Alamos National Laboratory, NM) were prepared by adding various amounts of 1 mM $^{65}Zn^{2+}$ (0.01–0.02 μ Ci/ μ l). Transport reactions were initiated by adding 0.225 ml of prewarmed (37 °C) buffer to .025 ml of cell suspension in a 37 °C water bath. After various times, the reaction tubes were removed from the water bath and immediately placed in ice to stop the transport reaction. Cell suspensions were rapidly filtered on GF/C filter paper using a Brandel cell harvester and washed 3 times with ice-cold buffer containing 137 mM cholineCl/10 mM Hepes, pH 7.4/1 mM EGTA. When initial velocity experiments were performed, the transport reactions were stopped by filtration. The radioactivity caught on the filters was determined by liquid scintillation counting. As total Zn^{2+} added to the buffers was known ($^{65}Zn^{2+}$ plus nonradioactive Zn^{2+}), aliquots of the uptake buffer were counted for radioactivity to determine the specific activity of $^{65}Zn^{2+}$. Using this value, the counts on the filter were converted to nanomoles of Zn^{2+} per milligram protein.

SNARF-1 fluorescence and acidification

K562 cells attached to poly-D-lysine coated glass coverslips were loaded with SNARF-1 by incubation for 30 min in Locke's buffer (pH 7.4) at 37 °C containing 5 μ M 5-(and-6)-carboxy SNARF-1, acetoxymethyl ester, acetate (Molecular Probes, Eugene, OR) [17]. The cells were then washed with 1 ml of Locke's buffer prior to pH measurement. The cells were then placed on ice until being used for an experiment. Cells attached to coverslips were held in a cuvette at approximately a 45° angle to the incident light beam by a coverslip holder (Hitachi Instruments, San Jose, CA). To measure fluorescence changes, the cuvette/coverslip holder was placed in the fluorescence spectrophotometer (Hitachi F-2000). To switch buffer solutions, the coverslip and holder were lifted out of the cuvette and quickly placed into a waiting cuvette containing the next desired buffer. SNARF-1 fluorescence was measured using excitation at 514 nm and emission wavelengths of 585 and 630 nm. The fluorescence ratio F_{585}/F_{630} was calibrated in separate experiments using cells treated with 10 μ M nigericin in Locke's buffer of various pH containing 120 mM KCl. Using the calibration data, intracellular pH was calculated directly from F_{585}/F_{630} . F_{585}/F_{630} was a linear function of pH over pH values between 6.4 and 8.0. In each experiment, to correct for scattered light/autofluorescence, data obtained from cells treated as above but without SNARF-1 incubation were subtracted from data obtained with SNARF-1 incubation.

ZnAF-2F fluorescence

K562 cells attached to poly-D-lysine coated glass coverslips were loaded with ZnAF-2F by incubation for 60 min in Locke's buffer (pH 7.4) at 37 °C containing 5 μ M ZnAF-2F

diacetyl ester [21]. The cells were then placed in fresh Locke's buffer and incubated at 37°C for an additional 30 min. Finally, the cells were placed on ice until used for an experiment. ZnAF-2F fluorescence changes were measured using excitation at 492 nm and emission at 524 nm. Data points were collected at various intervals and saved to a data file. Since ZnAF-2F is not a ratiometric probe, fluorescence data is presented as $\Delta F/F_0$. F_0 is the average fluorescence intensity obtained for each coverslip during a brief preincubation (20–90 s) in Locke's buffer (pH 6 or 8) without added Zn^{2+} . After preincubation, an experimental run was initiated by the addition of various solutions (e.g., Zn^{2+} , CaEDTA, and dH_2O) to the cuvette via a port in the coverslip holder. Opening the door to the cuvette chamber caused a brief disturbance in the recorded data. These data points were deleted and usually amounted to about 2–5 s of data. To calculate $\Delta F/F_0$, F_0 was subtracted from each data point ($=\Delta F$) and was normalized using F_0 ($=\Delta F/F_0$). ZnAF-2F (10 mM in DMSO) was mixed with an equal volume of pluronic acid (20% in DMSO, Molecular Probes) just before use and added with the appropriate dilution in Locke's buffer to obtain the desired final concentration for incubation with cells.

Correction for photodecay

Many experiments using ZnAF-2F required long incubations (up to 1 h), thus a correction for fluorescence changes due to photodecay was necessary. First, we determined the changes in intracellular pH occurring when cells were placed in pH 6 or 8 buffers (intracellular pH dropped from about 7.5 to about 6.7, measured with SNARF-1 fluorescence). The results can be seen in the inset to Fig. 1.

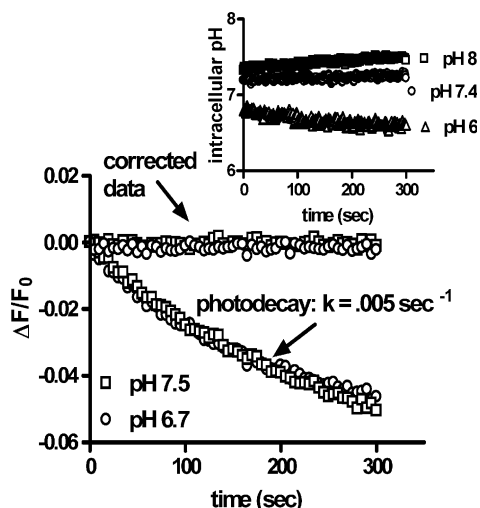


Fig. 1. Analysis of photodecay of ZnAF-2F and the effect of pH. ZnAF-2F free acid (1 μ M) was added to 1 μ M $ZnCl_2$ (10 mM HEPES) and then fluorescence recorded to observe the photodecay effect. Experiments were performed at either pH 7.5 or 6.7, which were intracellular pH values determined for conditions in this study. For ZnAF-2F results, data are from replicate experiments. Inset: intracellular pH was determined in K562 erythroleukemia cells preincubated with 5 μ M SNARF-1 and then placed into either pH 8, 7.4, or 6 Locke's buffer. Intracellular pH was estimated as described in Materials and methods.

Fig. 1 shows that the fluorescence signal decay was fit by a one phase exponential curve. K_{decay} and span were estimated from the decay data (see Fig. 1) using non linear curve fitting (GraphPad Prism ver 4, GraphPad Software, San Diego, CA) to the equation: $y = span \cdot \exp(-K \cdot x) + plateau$. $\Delta F/F_0$ values calculated from raw data were corrected at each time point for decay using the equation: fraction remaining = $e^{-K \cdot time}$. The fraction remaining was subtracted from 1 and multiplied by the span to obtain the correction factor, which was then added to $\Delta F/F_0$ at each time point. The net effect of the correction was to level the fluorescence signal over time (see Fig. 1). No effect of pH was seen on the decay rate. As the decay rate varied slightly from experiment to experiment, each experiment was corrected with its own decay rate.

Results

Previous studies using cultured rat cortical neurons show a robust $^{65}Zn^{2+}$ uptake when cells are placed in buffers containing micromolar concentrations of $^{65}Zn^{2+}$. $^{65}Zn^{2+}$ uptake was inhibited by extracellular acidification and stimulated by intracellular acidification [17–20]. We hypothesized that proton effects are fundamental to the transport mechanism and suggested the mechanism responsible for $^{65}Zn^{2+}$ uptake in cortical neurons could be a Zn^{2+}/H^+ antiporter. In an attempt to identify the protein responsible for pH dependent Zn^{2+} uptake, we took advantage of the well characterized pH dependence of plasma membrane Zn^{2+} transport in cortical neurons to examine the pH dependence of the SLC39A1 protein. The SLC39A1 protein is a logical choice since the kinetic properties of $^{65}Zn^{2+}$ uptake in cortical neurons [17], mirror closely those of the SLC39 family of transporters [4,5]. To test the hypothesis that the SLC39A1 protein (the gene is expressed in the brain) mediates pH dependent $^{65}Zn^{2+}$ uptake, we studied K562 erythroleukemia cells. Importantly, antisense oligonucleotides directed against SLC39A1 expression show nearly complete inhibition of $^{65}Zn^{2+}$ uptake indicating that SLC39A1 expression is sufficient to account for endogenous $^{65}Zn^{2+}$ uptake in K562 cells [5].

The net accumulation of $^{65}Zn^{2+}$ in K562 erythroleukemia cells is inhibited by extracellular acidification

Fig. 2 shows the dependence of the initial velocity of $^{65}Zn^{2+}$ uptake at pH 8 on extracellular Zn^{2+} concentration. The data were fit to a rectangular hyperbola ($y = V_{max} \cdot x / (K_m + x)$) using GraphPad Prism (ver 4) yielding estimates of 11 μ M for the K_m and 0.203 nmol/mg/s for the V_{max} . The inset to Fig. 2 shows that linear uptake is observed at least over the first 20 s at 30 μ M extracellular Zn^{2+} added. This is the amount of extracellular Zn^{2+} used in subsequent experiments. However, uptake did not extrapolate to zero uptake at zero time, but to about 0.8 nmol/mg. Zero time uptake was estimated by mixing ice cold cells with ice cold reaction buffer and immediately filtering the mix. The value obtained (0.78 nmol/mg at 30 μ M extracellular Zn^{2+}) matched the

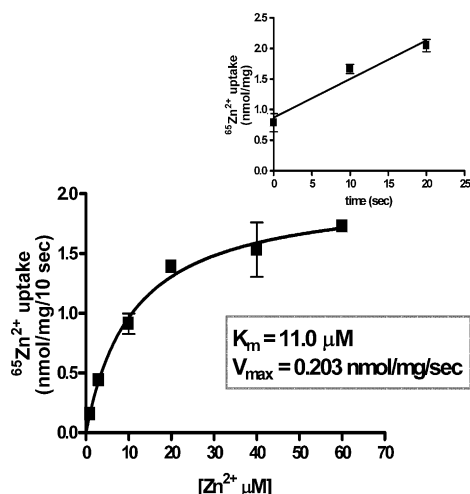


Fig. 2. Concentration dependence of the initial velocity of $^{65}\text{Zn}^{2+}$ uptake. K562 erythroleukemia cells were incubated at 37°C with either 1, 3, 10, 20, 40, or $60 \mu\text{M}$ $^{65}\text{Zn}^{2+}$ added, for 10 s. The reaction was stopped by immediately filtering the cell suspension followed with three washes of ice cold EGTA wash buffer (see Materials and methods). Inset: cells were treated as described above in $30 \mu\text{M}$ $^{65}\text{Zn}^{2+}$ for either 10 or 20 s before stopping the reaction. Zero time was estimated by mixing ice cold cells with ice cold buffer ($30 \mu\text{M}$ $^{65}\text{Zn}^{2+}$) and immediately filtering. Each point represents the mean \pm SEM of three replicate experiments.

extrapolated zero value, as can be seen in the inset. Zero time $^{65}\text{Zn}^{2+}$ uptake most likely represents plasma membrane bound and residual $^{65}\text{Zn}^{2+}$ caught on the filters that is resistant to removal by the cold wash buffer. This interpretation was confirmed when comparing $^{65}\text{Zn}^{2+}$ uptake data with ZnAF-2F fluorescence changes (see Fig. 4).

Figs. 3A and B show that during its initial phase, total $^{65}\text{Zn}^{2+}$ uptake was inhibited as much as 60% by changing the extracellular pH from 8 to 6, an effect similar to that seen in cortical neurons [17]. As a control (see Fig. 3A), it is shown that the inclusion of 1 mM CaEDTA completely inhibits $^{65}\text{Zn}^{2+}$ uptake (1 mM CaEDTA is typically used to chelate free extracellular Zn^{2+} because EDTA has a much higher affinity for Zn^{2+} than Ca^{2+} . Thus, free Zn^{2+} is lowered to picomolar levels, whereas free Ca^{2+} is barely affected.). The pH dependence of the initial uptake velocity

shows a smooth monophasic curve with an IC_{50} (pH 6.34) estimated from non linear curve fitting (GraphPad Prism ver 4). These data suggest that SLC39A1 protein transport function was inhibited by lowering extracellular pH.

In the presence of elevated extracellular Zn^{2+} , K562 erythroleukemia cells establish a new steady state with elevated free intracellular Zn^{2+} , shown with studies using the cell permeable fluorophore, ZnAF-2F DA, and $^{65}\text{Zn}^{2+}$

ZnAF-2F DA is a membrane permeable fluorophore with high affinity for Zn^{2+} , little pH sensitivity, and excellent selectivity over other divalent cations [21]. Fig. 4 shows fluorescence changes observed in K562 cells containing ZnAF-2F after addition of $30 \mu\text{M}$ Zn^{2+} compared to cells after an equal volume of water was added. When extracellular Zn^{2+} was increased a rising curvilinear trace was obtained, consistent with increasing intracellular free Zn^{2+} (see Fig. 4A). Intracellular free Zn^{2+} appeared to increase gradually until a new steady state was established, approximately 30 min after addition of Zn^{2+} .

As shown above, when K562 cells are placed in Zn^{2+} containing buffers, they accumulate significant amounts of $^{65}\text{Zn}^{2+}$ and show detectable ZnAF-2F fluorescence changes because of increased influx, but what is the relationship between these two measurements? Cellular Zn^{2+} content is determined by the relative rates of Zn^{2+} influx and efflux. When Zn^{2+} influx increases one expects an increase in cellular Zn^{2+} content. Conversely, when Zn^{2+} efflux increases, cellular Zn^{2+} content should decrease. When a steady state in free intracellular Zn^{2+} exists, influx and efflux are balanced and total cellular Zn^{2+} remains constant. In studies using ZnAF-2F, fluorescence changes are reporting changes in the free or easily exchangeable pools of intracellular Zn^{2+} . In studies using $^{65}\text{Zn}^{2+}$, changes in cellular $^{65}\text{Zn}^{2+}$ content can reflect plasma membrane binding, net uptake of $^{65}\text{Zn}^{2+}$, and equilibration of radioisotope with nonradioactive Zn^{2+} inside the cell (a reflection of $^{65}\text{Zn}^{2+}/\text{Zn}^{2+}$ exchange). We have shown that, after placing K562 cells in buffers containing micromolar added Zn^{2+} , influx is immediately increased. A net accumulation of Zn^{2+} occurs

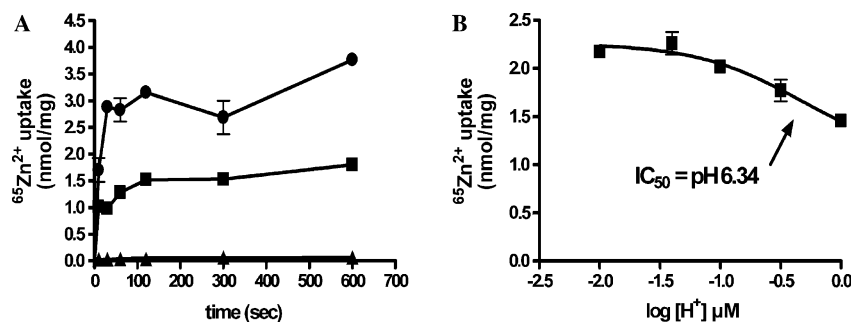


Fig. 3. Effect of pH and Zn^{2+} chelation by EDTA on $^{65}\text{Zn}^{2+}$ uptake measured in K562 erythroleukemia cells. (A) K562 erythroleukemia cells were incubated with $30 \mu\text{M}$ $^{65}\text{Zn}^{2+}$ for various times at pH 8 (\bullet), pH 6 (\blacksquare), or pH 8 containing 1 mM CaEDTA (\blacktriangle). (B) Uptake reactions were performed in buffer containing $30 \mu\text{M}$ $^{65}\text{Zn}^{2+}$ adjusted to various pH values between 8 and 6. $^{65}\text{Zn}^{2+}$ uptake reactions were stopped after 10 s at 37°C . Data were fit to the equation: $y = \text{bottom} + (\text{top} - \text{bottom}) / (1 + 10^{(x - \log \text{IC}_{50})})$ to estimate IC_{50} (GraphPad Prism ver 4). All data points are the means \pm SEM of at least three replicate experiments.

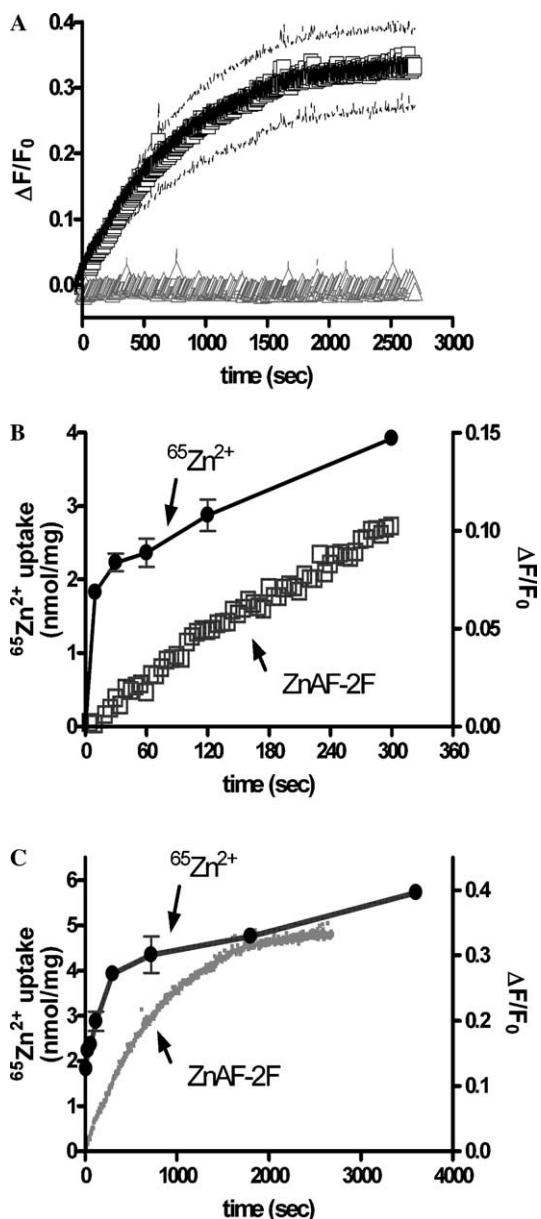


Fig. 4. ZnAF-2F fluorescence changes observed in K562 erythroleukemia cells exposed to increased extracellular Zn^{2+} . K562 erythroleukemia cells attached to glass coverslips were loaded with ZnAF-2F by incubation for 60 min in Locke's buffer (pH 7.4) at 37°C containing 5 μ M ZnAF-2F diacetyl ester. (A) Fluorescence intensity measured after either 30 μ M Zn^{2+} (\square), or an equal volume of water (Δ) was added to cells incubating in Locke's buffer pH 8 at 37°C. Each point represents the means \pm SEM (SEM represented as dotted line above and below the data points) of three replicate experiments. (B) Data from (A) (\square) are plotted on the same graph with data presented in Fig. 3A— $^{65}Zn^{2+}$ uptake in the presence of 30 μ M $^{65}Zn^{2+}$, pH 8 (\bullet). (C) Similar to (B) except data are plotted over a longer time frame (\square).

resulting in increasing $^{65}Zn^{2+}$ content and changes in ZnAF-2F fluorescence. Fig. 4B shows that during the initial phase of Zn^{2+} uptake the changes in ZnAF-2F fluorescence and $^{65}Zn^{2+}$ content parallel each other, but differ in that an initial rapid accumulation of $^{65}Zn^{2+}$ is seen. Analysis of initial rates of $^{65}Zn^{2+}$ uptake (Fig. 2) suggests that the initial burst in $^{65}Zn^{2+}$ accumulation is plasma membrane/filter

binding. The results of Fig. 4B agree with this interpretation. The transport reaction proceeds until a new steady state is attained (see Fig. 4C), as shown by both ZnAF-2F and $^{65}Zn^{2+}$ data. However, cellular $^{65}Zn^{2+}$ content will slowly continue to increase until the specific activity of $^{65}Zn^{2+}$ inside and outside the cell reaches equilibration, but likely results in little net change in cellular Zn^{2+} content.

The possibility exists that the plateau in ZnAF-2F fluorescence results from saturation or leakage of the dye, not establishment of a new steady state. We wanted to show that the leakage was in fact small and that the robustness of the intracellular dye response was well maintained even after long incubations. To show this, we used a Zn^{2+} ionophore (sodium pyrithione, -50μ M with 30 μ M Zn^{2+} added) added either at the start of a reaction or after a steady state had been achieved to maximally load the cells with Zn^{2+} . It can be seen in Fig. 5 that addition of sodium pyrithione results in a large and rapid rise in ZnAF-2F fluorescence when added at the start of the reaction, in response to a large influx of Zn^{2+} . After addition of 30 μ M Zn^{2+} alone a new steady state was established, however, addition of sodium pyrithione disturbed this steady state by allowing a rapid influx of additional Zn^{2+} , observed as increased ZnAF-2F fluorescence similar to that seen after addition at the start of the reaction. Thus, the establishment of a new steady state after addition of Zn^{2+} , reflected as a steady level of ZnAF-2F fluorescence, did represent a steady state in intracellular free Zn^{2+} concentration and was not the result of fluorophore saturation or leakage from the cell.

Extracellular acidification inhibits Zn^{2+} influx

In Figs. 6A and B, the effects of extracellular acidification on ZnAF-2F fluorescence changes, with or without Zn^{2+} addition are shown. We saw that the initial rate of

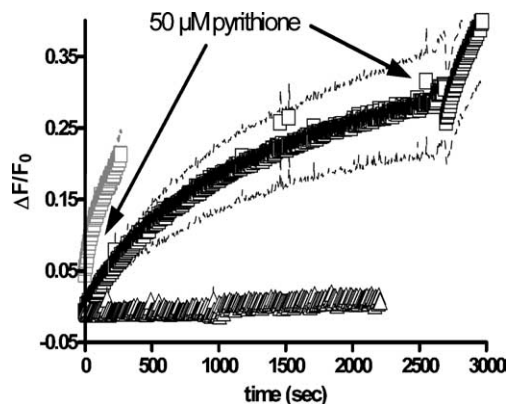


Fig. 5. ZnAF-2F fluorescence changes observed in K562 cells exposed to sodium pyrithione. K562 erythroleukemia cells attached to glass coverslips were prepared as described in the legend to Fig. 4 (30 μ M Zn^{2+} added to start the reaction \square ; or an equal volume of water Δ). At the indicated times, (see arrows), 50 μ M sodium pyrithione was added (pyrithione was not added to the water run). Data are means \pm SEM (SEM represented as dotted line above and below the data points) of three replicate experiments.

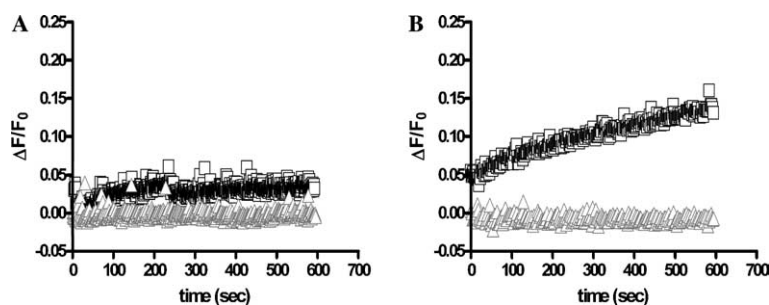


Fig. 6. ZnAF-2F fluorescence changes observed in K562 erythro leukemia cells exposed to extracellular acidification. K562 erythro leukemia cells attached to glass coverslips were prepared as described in the legend to fig. 4. (A) Cells were placed into pH 6 Locke's buffer and at time zero 30 μM Zn^{2+} (\square) or an equal volume of water (\triangle) was added. (B) Same as in (A) except that cells were in pH 8 Locke's buffer. All data represent means of at least duplicate experiments.

fluorescence increase observed after addition of 30 μM Zn^{2+} in pH 8 (see Fig. 6B), was almost completely blocked in pH 6 and differed little from that seen in the absence of added Zn^{2+} in either pH 8 or 6 (see Fig. 6A). We conclude that Zn^{2+} influx is inhibited (even in the presence of micromolar added extracellular Zn^{2+}) by extracellular acidification. Since the SLC39A1 protein is the primary, if not only, mediator of Zn^{2+} influx in K562 cells, we must conclude that SLC39A1 transport function is inhibited by extracellular acidification.

Discussion

The findings reported here demonstrate the effectiveness of using ZnAF-2F to monitor changes in intracellular Zn^{2+} and provide consistent evidence that Zn^{2+} influx in K562 erythro leukemia cells was inhibited by extracellular acidification. Our data shows that short term steady state levels of free intracellular Zn^{2+} are largely determined by the relative rates of Zn^{2+} influx and efflux across the plasma membrane. Our data is consistent with distinct pathways for Zn^{2+} influx (SLC39A1 protein mediated) and efflux. We show that under resting conditions, in Locke's buffer, K562 cells maintain a steady state with both Zn^{2+} influx (and presumably efflux) so small as to be undetectable by the methods employed in this study. Zn^{2+} influx is likely small because the contaminating concentration of free Zn^{2+} in Locke's buffer is below the activation level required to stimulate Zn^{2+} influx. Adding micromolar amounts of Zn^{2+} to the Locke's buffer clearly stimulated Zn^{2+} influx. Efflux is small under these conditions because free intracellular Zn^{2+} is small as well.

When Zn^{2+} influx was stimulated, cellular Zn^{2+} rose, and presumably free intracellular Zn^{2+} rose until a new steady state was attained. This study provides evidence that transported $^{65}\text{Zn}^{2+}$ readily equilibrated with free intracellular Zn^{2+} . We showed that over relatively short periods of time (up to one hour in this study) free intracellular Zn^{2+} was allowed to increase in response to changes in Zn^{2+} influx. Presumably, under either physiological or pathological conditions, if Zn^{2+} were released from intracellular sequestration sites, a transient rise in free intracellular Zn^{2+} would occur also. Such a rise in free intracellular Zn^{2+} has been

shown to occur in neurons after oxidative stress [22,23]. On the other hand, it is thought that long term cellular Zn^{2+} status and presumably free intracellular Zn^{2+} concentrations are regulated by the altered expression of SLC30A1 (Zn^{2+} efflux) and metallothionein [24,25] and the cycling of SLC39 proteins (Zn^{2+} influx) between the *trans*-Golgi network and the plasma membrane [6,26].

But does a free pool of intracellular Zn^{2+} even exist in eukaryotic cells? O'Halloran and co-workers [27,28] make the convincing argument that at least in *Escherichia coli*, metal binding proteins are so effective as to lower free intracellular Zn^{2+} and other metals to femtomolar levels. In eukaryotic cells, glutathione, and free amino acids (e.g., histidine) can act as additional Zn^{2+} binding moieties in addition to metallothionein/thionein pair [29,30]. Although these compounds have low affinity for Zn^{2+} , they exist in millimolar concentrations in the cell and are predicted to lower free intracellular Zn^{2+} to negligible levels. Thus, the Zn^{2+} signal sensed by ZnAF-2F might actually exist as a freely exchangeable (low affinity, bound) pool of Zn^{2+} , such that free Zn^{2+} actually changes little or not at all in our experiments.

This study adds to our growing knowledge of the transport mechanism of SLC39 proteins. SLC39 proteins are responsible for influx and appear to function by facilitated transport, dependent on a concentration gradient to provide the free energy for net movement of Zn^{2+} into the cell. This study provides evidence that SLC39A1 protein transport function is inhibited by extracellular acidification. The pH dependence of SLC39A1 protein transport activity has not been extensively studied [4,5], although the SLC39A2 protein was shown to be activated by bicarbonate ion. We took great care to eliminate bicarbonate effects by using bicarbonate free buffers bubbled with O_2 . Thus, we conclude that SLC39A1 protein transport activity is inhibited by extracellular acidification and this effect is not mediated through changes in bicarbonate ion. The IC_{50} of the pH effect is remarkably close to the amino acid histidine ($\text{p}K_a = 6.0$), suggesting histidine residues in the protein could play a critical role in the mechanism of pH effects. Sequence analysis of the SLC30 gene family [1] reveals a highly conserved histidine rich domain in the large intracellular loop between

transmembrane domains III and IV (albeit the function of this loop is unclear at present). In addition, transmembrane domains IV–V, which are predicted to be involved in Zn²⁺ translocation, contain histidine residues also. Thus, conserved histidine residues present in SLC39A1 that play a critical role in Zn²⁺ influx may be involved in the pH effect. Finally, it appears likely that the previously reported pH effect on Zn²⁺ transport in cortical neurons [17] is mediated through SLC39A1 protein activity.

Acknowledgments

This work was supported by a grant from the National Institute on Aging and the Provost's Undergraduate Research Fund at OHIO University.

References

- [1] D.J. Eide, Pflugers Arch. 447 (2004) 796–800.
- [2] L.A. Gaither, D.J. Eide, BioMetals 14 (2001) 251–270.
- [3] R.D. Palmiter, L. Huang, Pflugers Arch. 447 (2004) 744–751.
- [4] L.A. Gaither, D.J. Eide, J. Biol. Chem. 276 (2001) 22258–22264.
- [5] L.A. Gaither, D.J. Eide, J. Biol. Chem. 275 (2000) 5560–5564.
- [6] B.E. Kim, F. Wang, J. Dufner-Beattie, G.K. Andrews, D.J. Eide, M.J. Petris, J. Biol. Chem. 279 (2004) 4523–4530.
- [7] K. Wang, B. Zhou, Y.M. Kuo, J. Zemansky, J.A. Gitschier, Am. J. Hum. Genet. 71 (2002) 66–73.
- [8] R.B. Franklin, J. Ma, J. Zou, Z. Guan, B.I. Kukoyi, P. Feng, L.C. Costello, J. Inorg. Biochem. 96 (2003) 435–442.
- [9] R.D. Palmiter, S.D. Findley, EMBO J. 14 (1995) 639–649.
- [10] A.H. Kim, C.T. Sheline, M. Tian, T. Higashi, R.J. McMahon, R.J. Cousins, D.W. Choi, Brain Res. 886 (2000) 99–107.
- [11] L. Huang, C.P. Kirschke, J. Gitschier, J. Biol. Chem. 277 (2002) 26389–26395.
- [12] T. Kambe, H. Narita, Y. Yamaguchi-Iwai, J. Hirose, T. Amona, N. Sugiura, R. Sasaki, K. Mori, J. Biol. Chem. 277 (2002) 19049–19055.
- [13] S.L. Kelleher, B. Lonnerdal, J. Nutr. 132 (2002) 3280–3285.
- [14] C.P. Kirschke, L. Huang, J. Biol. Chem. 278 (2003) 4096–4102.
- [15] R.D. Palmiter, T.B. Cole, S.D. Findley, EMBO J. 15 (1996) 1784–1791.
- [16] R.D. Palmiter, T.B. Cole, C.J. Quaipe, S.D. Findley, Proc. Natl. Acad. Sci. USA 93 (1996) 14934–14939.
- [17] R.A. Colvin, Am. J. Physiol. Cell Physiol. 282 (2002) C317–C329.
- [18] R.A. Colvin, N. Davis, R.W. Nipper, P.A. Carter, Neurochem. Int. 36 (2000) 539–547.
- [19] R.A. Colvin, Neurosci. Lett. 247 (1998) 147–150.
- [20] R.V. Balaji, R.A. Colvin, Neurochem. Res. 30 (2005) 171–176.
- [21] T. Hirano, K. Kikuchi, Y. Urano, T. Nagano, J. Am. Chem. Soc. 124 (2002) 6555–6562.
- [22] E. Aizenman, A.K. Stout, K.A. Hartnett, K.E. Dineley, B. McLaughlin, I.J. Reynolds, J. Neurochem. 75 (2000) 1878–1888.
- [23] E. Bossy-Wetzel, M.V. Talantova, W.D. Lee, M.N. Scholzke, A. Harrop, E. Mathews, T. Gotz, J. Han, M.H. Ellisman, G.A. Perkins, S.A. Lipton, Neuron 41 (2004) 351–365.
- [24] S.J. Langmade, R. Rauind, P.J. Daniels, G.K. Andrews, J. Biol. Chem. 275 (2000) 34803–34809.
- [25] G.K. Andrews, Biochem. Pharmacol. 59 (2000) 95–104.
- [26] F. Wang, J. Dufner-Beattie, B.E. Kim, M.J. Petris, G.K. Andrews, D.J. Eide, J. Biol. Chem. 279 (2004) 24631–24639.
- [27] L.A. Finney, T.V. O'Halloran, Science 300 (2003) 931–936.
- [28] C.E. Outten, T.V. O'Halloran, Science 292 (2001) 2488–2492.
- [29] A. Krezel, J. Wojcik, M. Maciejczyk, W. Bal, W. May, Chem. Commun. (Camb.) 6 (2003) 704–705.
- [30] W. Maret, J. Nutr. 133 (2003) 1460S–1462S.